

# Mapping of continuum and lattice models for describing the adsorption of an ideal chain anchored to a planar surface

A. A. Gorbunov

*State Research Institute for Highly Pure Biopreparations, 7 Pudozhskaya, 197110 St. Petersburg, Russia*

A. M. Skvortsov

*Chemical-Pharmaceutical Academy, Prof. Popova 14, 197022 St. Petersburg, Russia*

J. van Male and G. J. Fleer

*Laboratory for Physical Chemistry and Colloid Science, Wageningen University, Dreijenplein 6, 6703 HB Wageningen, The Netherlands*

(Received 11 July 2000; accepted 14 December 2000)

An ideal polymer chain anchored to a planar surface is considered by using both lattice and continuum model approaches. A general equation relating the lattice and continuum model adsorption interaction parameters is derived in a consistent way by substituting the exact continuum solution for the free chain end distribution function into the lattice model boundary condition. This equation is not mathematically exact but provides excellent results. With the use of this relation the quantitative equivalence between lattice and continuum results was demonstrated for chains of both infinite and finite length and for all three regimes corresponding to attractive, repulsive and adsorption-threshold energy of polymer-surface interaction. The obtained equations are used to discuss the distribution functions describing the tail of an anchored macromolecule and its adsorbed parts. For the tail-related properties the results are independent of the microscopic details of the polymer chain and the adsorbing surface. One interesting result obtained in the vicinity of adsorption threshold point is a bimodal tail length distribution function, which manifests chain populations with either tail or loop dominance. The properties related to the number of surface contacts contain, apart from universal scaling terms, also a nonuniversal factor depending on microscopic details of polymer-surface interaction. We derived an equation for calculating this nonuniversal factor for different lattice models and demonstrated excellent agreement between the lattice results and the continuum model. © 2001 American Institute of Physics.

[DOI: 10.1063/1.1346686]

## I. INTRODUCTION

Understanding the behavior of an ideal flexible-chain polymer anchored to a planar surface is important for both basic research and applications. The fundamental interest derives from the fact that this is an exactly solvable problem giving a phase transition.<sup>1,2</sup> However, this system also serves as a model for more applied phenomena and processes such as adsorption of polymers from solution, flocculation, and stabilization of colloids by polymers, polymer fractionation by chromatography, etc.<sup>3-9</sup> This problem was studied extensively in early papers<sup>10-15</sup> but also more recently; reviews on these theoretical aspects can be found in Refs. 3 and 16-18.

The most simple and straightforward way to model a polymer molecule in solution and its interaction with a surface is based on lattice random walks. Such lattice models were used in the basic papers<sup>10-15</sup> and in several extensions, including Monte Carlo studies of chains with excluded volume.<sup>19-21</sup> Lattice models can be easily generalized to describe more complex polymer systems.<sup>3</sup> Unfortunately, such models contain parameters which are lattice dependent, and therefore it is often difficult to see the universal features in lattice results and to make a quantitative comparison with experiments.

The other popular technique is based on the continuum

approach<sup>16,17,21-24</sup> which is analogous to describing the motion of a Brownian particle near a surface. The model parameters in the continuum description are related only to large-scale spatial properties, such as the average radius of a polymer molecule far from the surface and the average thickness of a macromolecule adsorbed on a surface. These continuum models are largely universal and independent of the microscopic structure of a surface layer and the details of the adsorption interaction potential.

The qualitative equivalence between lattice and continuum models is well established.<sup>1,16,17,21-26</sup> However, so far it was difficult to make a quantitative comparison since no general relation between the adsorption interaction parameters in the lattice and continuum models was available. Different relations obtained in the thermodynamic limit of a long chain have been proposed and applied in Refs. 25-27.

The objective of this paper is to derive in a consistent way a more general relation between the lattice and continuum model adsorption interaction parameters and to demonstrate the quantitative equivalence between lattice and continuum results for an ideal chain anchored to a planar surface. Since the mathematical forms of the known solutions for the lattice and continuum models are very different, we cannot expect a mathematically exact parameter map-

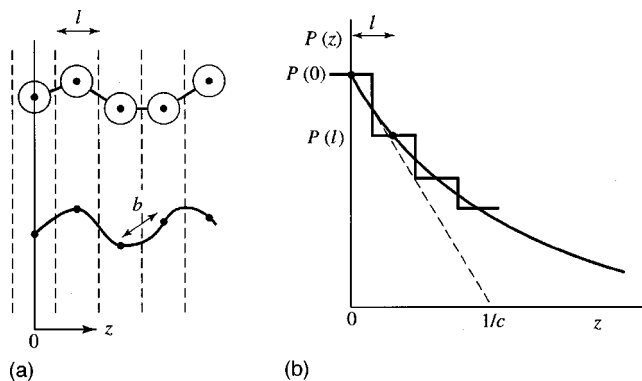


FIG. 1. (a) Lattice and continuum representations of an end-attached chain. In the lattice version the segments are restricted to positions  $z=0, l, 2l, \dots$ , where  $l$  is the lattice spacing. Segments in layer 0 experience an adsorption energy  $-\chi_s$ . In the continuum model the chain is a continuum curve with contour length  $Nb$ ; all points of the curve can visit the region  $z>0$ . The ratio between  $b$  and  $l$  is  $\sqrt{6\lambda}$  where  $\lambda$  is the lattice parameter. (b) End-point distribution  $P(z, N)$  of an adsorbing chain of  $N$  segments in the continuum model (smooth curve) and in the lattice (steps). The extrapolation length (average layer thickness) is  $1/c$ , where  $c$  is large for strong adsorption and zero in the critical point. The relation between  $c$  and  $\chi_s$  is found from  $P(0, N)$ ,  $P(0, N+1)$ , and  $P(l, N)$ , according to Eq. (13).

ping. However, we will show how this mapping can be carried out to give essentially (and quantitatively) the same physics for both models.

In addition we will discuss two important distribution functions, related to the number of adsorbed and tail segments. These functions have not been investigated in detail before.

## II. LATTICE MODEL

We consider a polymer chain lattice model (Fig. 1) characterized by a lattice parameter  $\lambda$ , which is the transition probability for a step from a given layer to an adjacent layer. In a simple cubic lattice  $\lambda=1/6$ . The center of adsorbed segments is situated at  $z=0$ , and nonadsorbed segments are at  $z=l, 2l, \dots$ , where  $l$  is the thickness of a lattice layer. Hence the anchored chain starts at  $z=0$ .

In order to account for segmental adsorption in such models a short-ranged attractive potential is usually introduced acting on the chain units at  $z=0$ . The adsorption interaction parameter  $\chi_s$  is defined as minus the free energy change of a chain unit due to formation of a contact between this unit and a surface. We express all the energy parameters in units of  $kT$ . An important characteristic, which depends on the lattice type, is the critical value of the adsorption parameter

$$\chi_{sc} = -\ln(1-\lambda). \tag{1}$$

Adsorption of a long chain in the absence of an external field starts when  $\chi_s$  exceeds the value  $\chi_{sc}$ . For the simple cubic lattice  $\chi_{sc} = \ln(6/5)$ .

The statistical weight  $P(z, n)$  for a chain part of  $n$  units to end in layer  $z>0$  from the surface obeys the well-known recurrence equation introduced by Rubin:<sup>15</sup>

$$P(z, n+1) = \lambda P(z-l, n) + (1-2\lambda)P(z, n) + \lambda P(z+l, n) \quad \text{for } 1 \leq n \leq N, \tag{2}$$

where  $N$  is the total number of chain segments. Equation (2) is the zero-field version of the more general theory of Scheutjens and Fleer.<sup>3,28</sup>

The boundary condition, which is equivalent to the recurrence equation for adsorbed segments which are at  $z=0$  and experience an adsorption energy  $-\chi_s$ , has the form:

$$P(0, n+1) = \exp(\chi_s)[(1-2\lambda)P(0, n) + \lambda P(l, n)]. \tag{3}$$

Because  $P(z, n)$  is zero for negative  $z$ , the term  $P(-l, n)$  is absent. The initial condition corresponding to the chain grafting is represented by

$$P(0, 1) = \exp(\chi_s), \tag{4}$$

$$P(z, 1) = 0 \quad \text{for } z>0$$

which expresses that the first segment can only start from  $z=0$ .

Analytical solutions of the problem as formulated in Eqs. (2)–(4) in the limit of an infinitely long chain are well known.<sup>15</sup> For finite lengths of the chain the results are usually obtained numerically.

## III. CONTINUUM MODEL

The continuum description is based on a model which is analogous to describing the trajectory of a Brownian particle in the presence of a planar surface. Only the direction  $z$  normal to the surface is of interest here, since the motion in the  $x-y$  plane parallel to the surface is free and is described by the usual Gaussian functions. One end of the chain with contour length  $Nb$ , where  $b$  is the segment length, is again anchored at  $z=0$ . The statistical weight  $P(z, n)$  of a chain section of contour length  $nb$  ending at coordinate  $z$  satisfies the diffusion equation:<sup>29</sup>

$$\frac{\partial}{\partial n} P(z, n) - \frac{b^2}{6} \frac{\partial^2}{\partial z^2} P(z, n) = 0. \tag{5}$$

Obviously, both  $n$  and  $z$  are now not discretized but continuous:  $z \geq 0, 0 \leq n \leq N$ . This differential equation represents the continuum version of the recurrence equations (2) describing lattice random walks outside the surface layer.<sup>3</sup> Equations of the type of Eq. (5) are also well known for describing heat conduction phenomena and quantum mechanical problems (Schrödinger equation).

The adsorption interaction with the plane can be described through the boundary condition<sup>30</sup>

$$P^{-1} \frac{\partial}{\partial z} P \Big|_{z=0} = -c, \tag{6}$$

where  $c$  is the inverse of the so-called extrapolation length [see also Fig. 1(b)], and is related to the lattice adsorption energy parameter  $\chi_s$ . It is negative for  $\chi_s < \chi_{sc}$ , zero at  $\chi_s = \chi_{sc}$ , and positive for  $\chi_s > \chi_{sc}$ , increasing monotonously with  $\chi_s$ . The precise relation between  $c$  and  $\chi_s$ , which follows from comparing the boundary conditions Eqs. (3) and (6) in the two models, is given in Sec. IV.

The boundary condition (6) is the same as the one appearing for the stationary Schrödinger equation in the presence of a  $\delta$ -functional pseudopotential. Mathematically, adsorption corresponds to the existence of bound states in the quantum-mechanical problem. It is well known that in the strong adsorption regime (for sufficiently large and positive  $c$  or  $\chi_s - \chi_{sc}$ ) the end-point distribution (which generally can be written as an eigenfunction expansion) is dominated by the lowest (ground-state) eigenvalue.<sup>1</sup> This distribution then becomes expressible in terms of this ground-state eigenvalue and the corresponding ground-state eigenfunction only.

The interaction is assumed to be short ranged with a characteristic length scale of order  $b$ . Negative  $c$  values correspond to effective repulsive forces. As stated above, the point  $c=0$ , at which the adsorption of an infinitely long chain starts, corresponds to  $\chi_s = \chi_{sc}$  in the lattice model and this point is usually referred to as a multicritical point.<sup>2,16,31</sup> Positive values of  $c$  correspond to adsorption and therefore  $c$  may be considered as an adsorption parameter. Its inverse  $1/c$  is the average thickness of the layer formed by an adsorbed macromolecule on the surface (see Fig. 1). The parameter  $c$  has the dimension of inverse length. It turns out to be convenient to use also a dimensionless adsorption parameter in the continuum model. Therefore we define a dimensionless interaction parameter  $C$  by

$$C \equiv \frac{bc}{\sqrt{6}}. \quad (7)$$

An analytical expression for the function  $P$ , satisfying Eq. (5) with the boundary condition (6), was obtained in Ref. 22 (see also Ref. 21). This solution for a chain of  $N$  units can be written as

$$P(z, N, C) = \frac{1}{2R\sqrt{\pi}} e^{-\zeta^2} [1 + \sqrt{\pi}\gamma \cdot Y(\zeta - \gamma)], \quad (8)$$

where the parameters  $R$ ,  $\zeta$ , and  $\gamma$  are defined as

$$R = b\sqrt{\frac{N}{6}}, \quad \zeta \equiv \frac{z}{2R}, \quad \gamma \equiv cR \equiv C\sqrt{N}.$$

Here  $R$  is the radius of gyration of a free Gaussian chain, and  $\zeta$  is the scaled, dimensionless distance of the chain end from the surface. The dimensionless parameter  $\gamma$  is a scaled adsorption interaction parameter. The function  $Y(x)$  is related to the well-known complementary error function  $\operatorname{erfc}(x)$ :

$$Y(x) = e^{x^2} \cdot \operatorname{erfc}(x)$$

$$Y(x) \approx \begin{cases} \frac{1}{\sqrt{\pi}} \left( \frac{1}{x} - \frac{1}{2x^3} + \frac{1 \cdot 3}{2^2 x^5} - \dots \right) & \text{at } x \gg 1, \\ 1 - \frac{2}{\sqrt{\pi}} x + x^2 - \frac{4}{3\sqrt{\pi}} x^3 + \dots & \text{at } |x| \ll 1, \\ 2e^{x^2} + \frac{1}{\sqrt{\pi}x} & \text{at } -x \gg 1. \end{cases} \quad (9)$$

The expansions of  $Y(x)$  in different regimes are shown in the latter three equations. With these limiting forms the qualitative features of the end-point distribution  $P(z, N, C)$  are eas-

ily found. Around the critical point ( $\gamma=0$ ) the end-point distribution is almost Gaussian. In the depletion region (negative  $\gamma$ ) this distribution is also of a Gaussian type:  $P \propto [\zeta/(\zeta - \gamma)] \exp(-\zeta^2)$ . However, in the strong adsorption region the distribution becomes exponential:  $P \propto \exp(-2\zeta\gamma) = \exp(-cz)$ , corresponding to the ground-state regime.

The integral of the function  $P$  over all positions of the free end gives the partition function  $Q(N, C)$  for an anchored polymer chain of  $N$  units with adsorption energy parameter  $C$ :

$$Q(N, C) = \int_0^\infty P(z, N) dz = Y(-\gamma). \quad (10)$$

Hence, the partition function  $Q$  depends not on the two separate parameters  $N$  and  $C$ , but only on the product  $\gamma \equiv C\sqrt{N}$ .

In the limiting case of large positive  $C$  ( $C \gg N^{-1/2}$  or  $\gamma \gg 1$ ), Eq. (10) for the partition function reduces to the exponential function

$$Q(N, C) \approx 2e^{\gamma^2} = 2e^{C^2 N}. \quad (11)$$

The condition  $\gamma \gg 1$  corresponds to the ground-state regime, and  $C^2$  in this case represents the ground-state eigenvalue.

At  $-\gamma \gg 1$  (large negative  $C$ ) the partition function takes the form

$$Q(N, C) \approx \frac{1}{\sqrt{\pi(-\gamma)}} = \frac{1}{(-C)\sqrt{\pi N}}. \quad (12)$$

#### IV. RELATION BETWEEN THE ADSORPTION INTERACTION PARAMETERS OF THE CONTINUUM AND LATTICE MODELS

For the special case of critical conditions ( $C=0$  in the continuum model) for infinitely long chains, Weiss and Rubin, and Rubin (Ref. 18) discussed the applicability of reflecting boundary conditions in this case. The condition  $C=0$  then corresponds to  $\chi_s = \chi_{sc}$  in the lattice model, where  $\chi_{sc}$  is defined in Eq. (1). These authors did not give a relation between  $C$  and  $\chi_s$  outside the critical point, or for finite chain lengths.

Approximate equations relating the adsorption parameters  $C$  and  $\chi_s$  for a long polymer chain have been discussed previously by Gorbunov and Skvortsov<sup>25</sup> and by Fleer *et al.*<sup>26</sup> In Ref. 26 only the adsorption case was considered, in Ref. 25 the case of strong repulsion was discussed as well. Although the approaches used in Refs. 25 and 26 are quite different, both are based upon the assumption  $|C|\sqrt{N} \gg 1$ , which means either sufficiently large chain length (large  $N$ ), or  $\chi_s$  values relatively far from the multicritical point  $\chi_s = \chi_{sc}$  (i.e.,  $C=0$ ). Now we derive, in a consistent way, more general equations relating  $C$  and  $\chi_s$  for all  $N$  and adsorption interaction regimes.

In the lattice model the boundary condition is given by Eq. (3), which shows that the ratios  $P(0, N)/P(0, N+1)$  and  $P(l, N)/P(0, N+1)$  are fixed by the value of the segmental

adsorption energy parameter  $\chi_s$ . In the continuum model we have an expression for the distribution function  $P(z, N, C)$  which does not contain  $\chi_s$  but which depends on the continuum interaction parameter  $C$ . If we combine the two approaches, we find a relation between  $C$  and  $\chi_s$ . Thus we substitute  $P(z, N, C)$  according to Eq. (8) in the lattice boundary condition (3):

$$\chi_s = -\ln \left[ \frac{(1-2\lambda)P(0, N, C) + \lambda P(l, N, C)}{P(0, N+1, C)} \right]. \quad (13)$$

To this end we need a relation between  $l$  and  $b$ , which follows from equating the radius of gyration for a  $N$ -step continuum Gaussian chain,  $R = b\sqrt{N/6}$  to that of a lattice chain:  $R = l\sqrt{\lambda N}$ . Hence,

$$l = \frac{b}{\sqrt{6\lambda}} \quad (14)$$

which prescribes how the lattice spacing  $l$  should be adjusted in different lattices, taking the bond length  $b$  to be invariant.

In deriving Eq. (13), we substituted the known analytical continuum expression into the lattice boundary condition to find which value of  $\chi_s$  corresponds to a given  $C$ . In principle, the inverse procedure would also be possible, inserting the continuum boundary condition into the lattice recurrency relation. However, since there is no analytical representation of these recurrency relations, this would require a numerical procedure to find which  $C$  would correspond to a given  $\chi_s$ . The result is expected to be essentially the same as solving  $C$  implicitly from Eq. (13) for given  $\chi_s$ .

Formula (13) expresses  $\chi_s$  as a function of the parameter  $C$ , of the number of chain units  $N$ , and of the lattice parameter  $\lambda$ . Therefore the relation  $\chi_s(C)$  is obtained for every lattice type and any chain length.

Figure 2(a) shows this relation calculated for three values of  $\lambda$ : 1/6 (simple cubic lattice), 1/4 (hexagonal or tetrahedral lattice), and 1/3 which does not correspond to any geometrical lattice, but is sometimes used to minimize lattice artifacts.<sup>32</sup> For the simple cubic lattice with  $\lambda = 1/6$  the  $\chi_s(C)$  relations are plotted for two finite chain lengths:  $N = 10$  and  $N = 100$ , and also for the limiting case  $N \rightarrow \infty$ . For the other two  $\lambda$  values only the limiting relations corresponding to  $N \rightarrow \infty$  are plotted.

It can be seen in Fig. 2(a) that the limiting curves  $\chi_s(C)$  for different lattices have similar shapes, with  $\chi_s$  being a monotonously increasing function of  $C$ . For small  $N$  and negative  $C$  the relation  $\chi_s(C)$  deviates slightly from the limiting  $\chi_s(C)$  curve for infinite chain length, but this deviation practically disappears at  $N > 100$ . The effect of  $N$  is nearly absent in the adsorption regime. At sufficiently large positive  $C$  ( $C > N^{-1/2}$ ) the dependence on  $N$  completely vanishes.

Analytical approximations of the function  $\chi_s(C)$  for different regimes of interaction can be obtained by using the asymptotic expansions of Eq. (9). The result can be written as

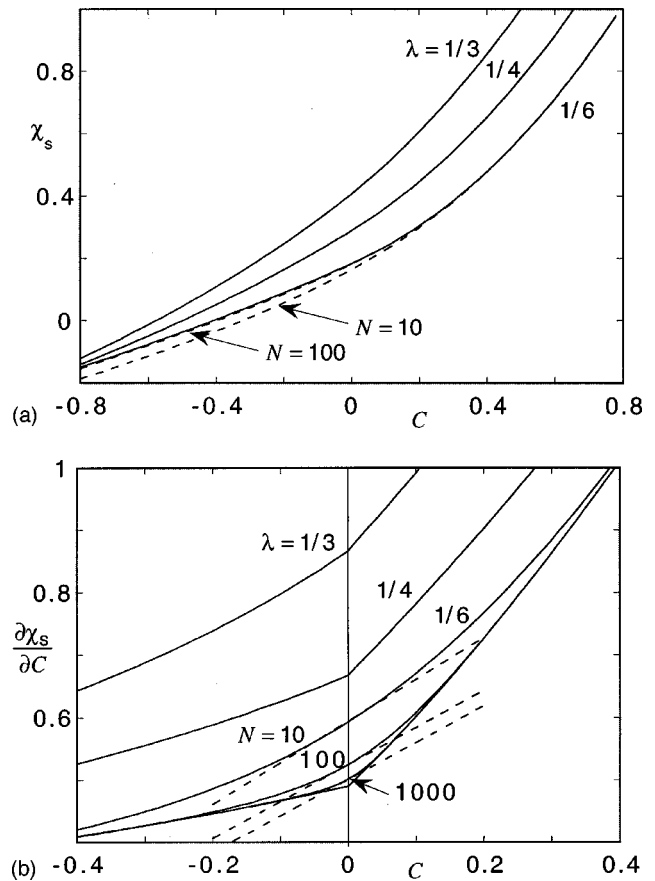


FIG. 2. (a) Relation between the continuum model interaction parameters  $C$  and the lattice adsorption energy  $\chi_s$ , for three lattice types:  $\lambda = 1/6, 1/4$ , and  $1/3$ . The full curves are for  $N \rightarrow \infty$ ; for  $\lambda = 1/6$  results for  $N = 10$  and  $N = 100$  are also given as dashed curves. (b) First derivative  $\partial \chi_s / \partial C$  as a function of  $C$  for the same lattice types. The three curves for  $N \rightarrow \infty$  show a kink at  $C = 0$ . For  $\lambda = 1/6$  three dependencies for finite  $N$  (10, 100, 1000) are also shown. Dashed lines represent the linear expansion around the point  $C = 0$  corresponding to Eq. (20).

$$\chi_s \approx \begin{cases} C^2 - \ln(1 - 2\lambda + \lambda e^{-C/\sqrt{\lambda}}) & C \gg \frac{1}{\sqrt{N}} \\ \chi'_{sc} + C \left( A_0 + \frac{A_1}{\sqrt{N}} + \frac{A_2}{N} \right) & |C| \ll \frac{1}{\sqrt{N}} \\ -\ln \left( 1 - \lambda - C\sqrt{\lambda} + \frac{3}{4} \frac{1-2\lambda}{N} \right) & -C \gg \frac{1}{\sqrt{N}} \end{cases} \quad (15)$$

where the constants  $A_0$ ,  $A_1$ , and  $A_2$  depend only on the lattice type, according to

$$A_0 = \frac{\sqrt{\lambda}}{1-\lambda}, \quad A_1 = \frac{\sqrt{\pi}(1-2\lambda)}{4(1-\lambda)}, \quad A_2 = \frac{4\lambda-1}{12\sqrt{\lambda}(1-\lambda)}.$$

The parameter  $\chi'_{sc}$  is defined as

$$\chi'_{sc} = \chi_{sc} - A_1 / (\sqrt{\pi N}) \quad (16)$$

and may be considered as the adsorption/desorption point ( $C = 0$ ) for finite chain lengths. Obviously, for  $N \rightarrow \infty$   $\chi'_{sc} = \chi_{sc}$ . For finite chain lengths  $\chi'_{sc} < \chi_{sc}$ , but the correction is small, as can be seen from Fig. 2(a). Nevertheless, Eq. (16)

gives explicitly the chain-length dependence of the adsorption transition, which is a new result. At  $N \rightarrow \infty$  Eq. (15) can be simplified:

$$\chi_s = \begin{cases} C^2 - \ln(1 - 2\lambda + \lambda e^{-C/\sqrt{\lambda}}), & C \geq 0, \\ -\ln[1 - \lambda - C\sqrt{\lambda}], & C \leq 0. \end{cases} \quad (17)$$

Equation (17) gives  $\chi_s$  as an explicit function of  $C$ . It is also useful to consider the inverse relation  $C(\chi_s)$ . The relation  $\chi_s(C)$  for the strong repulsion case may be inverted directly. This is not the case in the strong adsorption limit. For this regime Gorburnov and Skvortsov<sup>25</sup> derived an approximate analytical expression by comparing lattice and continuum expressions for the partition function  $Q$  at  $N \rightarrow \infty$ .

$$C = \begin{cases} \sqrt{-\ln(p) - \ln\left[1 - \frac{1}{2\lambda}\left(1 - \sqrt{1 + 4\lambda(1/p - 1)}\right)\right]}, \\ \sqrt{\lambda}(p - 1), & C \leq 0, \end{cases} \quad (18)$$

$C \geq 0$ ,

where  $p = (1 - e^{-\chi_s})/\lambda = (1 - e^{-\chi_s})/(1 - e^{-\chi_{sc}})$ .

Equations (17) and (18) coincide with the previous results of Refs. 25 and 26. Although the mathematical functions in the positive  $C$  region of Eq. (17) and Eq. (18) are quite different, the numerical results are virtually identical, with a maximum difference of less than 0.1%.

In the next section we shall need not only  $\chi_s(C)$ , but also the first derivative  $\partial\chi_s/\partial C$  as a function of  $C$  and  $N$ . The limiting form for this derivative at  $N \rightarrow \infty$  follows directly from Eq. (17) as

$$\frac{\partial\chi_s}{\partial C} \approx \begin{cases} 2C + \sqrt{\lambda}(\lambda + (1 - 2\lambda)e^{C/\sqrt{\lambda}})^{-1}, & C \geq 0, \\ \sqrt{\lambda}(1 - \lambda - C\sqrt{\lambda})^{-1}, & C \leq 0. \end{cases} \quad (19)$$

Hence, in this limit for infinite  $N$ ,  $\partial\chi_s/\partial C$  is continuous in the critical point ( $C=0$ ). For finite  $N$ ,  $\partial\chi_s/\partial C$  around  $C=0$  may be found by expanding the exact Eq. (13) in powers of  $C$ , using Eq. (8) with expansion (9) for the function  $Y(x)$ . The result is

$$\frac{\partial\chi_s}{\partial C} \approx A_0 + \frac{A_1}{\sqrt{N}} + \frac{A_2}{N} + C\left[B_0 + \frac{B_2}{N}\right], \quad (20)$$

where  $A_0$ ,  $A_1$ , and  $A_2$  were defined below Eq. (15) and

$$B_0 = 2 - \frac{1 - 2\lambda}{1 - \lambda} \left( \frac{\pi}{2} + \frac{\lambda}{1 - \lambda} \right),$$

$$B_2 = \frac{24 - 6\pi - \lambda(80 - 21\pi) + \lambda^2(80 - 15\pi)}{48\lambda(1 - \lambda)^3}.$$

The derivative  $\partial\chi_s/\partial C$  is plotted in Fig. 2(b) for several conditions. The lower four solid curves are the exact results for  $\lambda=1/6$  and  $N=10, 100, 1000$ , and  $10000$ . For finite  $N$  the curves are smooth around  $C=0$  but the curves for  $N \rightarrow \infty$ , given by Eq. (19), display a kink at  $C=0$ : the second derivative  $\partial^2\chi_s/\partial C^2$  is discontinuous in this case. Except for a small region around  $C=0$ , the curves for  $N=100$  and  $1000$  practically coincide with the limiting curve  $N \rightarrow \infty$ . For  $N=10$  the deviations are larger; nevertheless the curve approaches the limiting curve for large enough  $|C|$ .

The dashed straight lines in Fig. 2(b), giving the tangent at  $C=0$ , were calculated with the expanded form of Eq. (20). The two upper solid curves in Fig. 2(b) give the limiting curve ( $N \rightarrow \infty$ ) for  $\lambda=1/4$  and  $\lambda=1/3$ , respectively. The value of  $\partial\chi_s/\partial C$  is higher than for  $\lambda=1/6$ , but the qualitative features are the same. In order not to overcrowd the figure, we have not given the curves for finite  $N$  for these lattice types.

As discussed above, the limiting curve for  $\partial\chi_s/\partial C$  describes the dependence for finite  $N$  quite well except for  $C$  close to zero. The relative difference at  $C=0$  is, according to Eq. (20), approximately given by  $(A_1/A_0)N^{-1/2}$ :

$$\frac{\frac{\partial\chi_s}{\partial C} - \frac{\partial\chi_s}{\partial C}\Big|_{\infty}}{\frac{\partial\chi_s}{\partial C}\Big|_{\infty}} \approx \frac{1 - 2\lambda}{4} \sqrt{\frac{\pi}{\lambda N}} = \frac{\sqrt{\pi}(1 - 2\lambda)}{4} \frac{l}{R}. \quad (21)$$

This equation gives an estimate of the error in using the simple asymptotic equation (19) instead of the general equations (8), (13), and (14). It is interesting to note that the limiting equation (19) describes the derivative for finite  $N$  more accurately at high  $\lambda$  values. For example, according to Eq. (21) the largest difference between the derivatives for  $N=100$  and  $N \rightarrow \infty$  is equal to 7.2%, 4.4%, and 2.6% for the lattices with  $\lambda=1/6, 1/4$ , and  $1/3$ , respectively.

As noted above, the limiting  $\partial\chi_s/\partial C$  curves show a kink at  $C=0$ , which implies a discontinuity of the second derivative  $\partial^2\chi_s/\partial C^2$ . According to Eqs. (19) and (20), at  $N \rightarrow \infty$  the second derivative close to the point  $C=0$  is given by

$$\frac{\partial^2\chi_s}{\partial C^2} = \begin{cases} \frac{\lambda}{(1 - \lambda)^2}, & C = -0, \\ 2 - \frac{1 - 2\lambda}{1 - \lambda} \left( \frac{\pi}{2} - \frac{\lambda}{1 - \lambda} \right), & C = 0, \\ \frac{1 - 2\lambda + 2\lambda^2}{(1 - \lambda)^2}, & C = +0. \end{cases} \quad (22)$$

Equations (13)–(20) derived in this section give the opportunity to compare and to combine results obtained for continuum and different lattice models. In the remainder of the paper we shall use these equations to discuss the distribution functions describing the tail of an anchored macromolecule and its adsorbed parts (which are usually called trains in a lattice model or surface contacts in a continuum description).

## V. AVERAGE NUMBER OF SURFACE CONTACTS AND CONTACT NUMBER DISTRIBUTION FUNCTION

The average number of surface contacts  $\langle S \rangle$  is an important parameter, which has been extensively discussed in many papers for both lattice and continuum models of an anchored polymer chain.<sup>14–17</sup> However, up to now there is no direct comparison of the results obtained with lattice and continuum models.

The average scaled number of contacts  $\langle M \rangle$  in the continuum model was introduced and obtained by Eisenriegler

*et al.* in Ref. 21 from analyzing the monomer density profile in the region  $z \rightarrow 0$ . Their result can be written as

$$\langle M \rangle \equiv \frac{1}{2R} \frac{\partial \ln Q}{\partial c} = \gamma + \frac{1}{\sqrt{\pi} Y(-\gamma)}. \quad (23)$$

The authors assumed that the average number of contacts  $\langle S \rangle$  is proportional to  $2R\langle M \rangle = \partial \ln Q / \partial c$ . This is correct in the very vicinity of the multicritical point, where  $c$  is proportional to  $\chi_s$  [see Fig. 2(a)] but in general the proportionality coefficient depends strongly on  $c$ . If this is the case, differentiation with respect to  $c$  is not the proper procedure. Since each contact contributes an amount  $\chi_s$  to the free energy,  $\ln Q$  should be differentiated with respect to  $\chi_s$ :

$$\langle S \rangle = \frac{\partial \ln Q}{\partial \chi_s} = \frac{\partial c}{\partial \chi_s} 2R \langle M \rangle. \quad (24)$$

For the average fraction of surface contacts  $\langle s \rangle \equiv \langle S \rangle / N$  we thus obtain

$$\begin{aligned} \langle s \rangle &= \frac{b^2}{3R} \cdot \frac{\partial c}{\partial \chi_s} \cdot \left[ \gamma + \frac{1}{\sqrt{\pi} Y(-\gamma)} \right] \\ &= \frac{2}{\sqrt{N}} \cdot \frac{\partial c}{\partial \chi_s} \cdot \left[ \gamma + \frac{1}{\sqrt{\pi} Y(-\gamma)} \right]. \end{aligned} \quad (25)$$

It is interesting to note that  $\langle s \rangle$  depends on the lattice type since the factor  $\partial c / \partial \chi_s$  contains the dependence on  $\lambda$ . Although the presence of a nonuniversal scaling factor for the number of surface contacts was mentioned in Ref. 33, the dependence of this factor on the parameters  $C$ ,  $N$ , and  $\lambda$  has not been investigated so far.

In the preceding section we discussed both general and approximate formulas [Eqs. (13)–(20)] for the parameter  $\chi_s$  and the derivative  $\partial \chi_s / \partial C$  as a function of  $C$  and  $N$  [see also Figs. 2(a) and 2(b)]. Using these results and Eq. (25) it is possible to calculate the dependence of  $\langle s \rangle$  on  $C$  for any chain length  $N$  and lattice parameter  $\lambda$ . Below we give simple approximate formulas for the average fraction of contacts  $\langle s \rangle$ . For the ground-state regime ( $\gamma \gg 1$ ) we have for long enough chains ( $N > 10$ ):

$$\langle s \rangle \approx \left( 1 + \frac{\sqrt{\lambda}}{2C} \cdot \frac{1}{(1-2\lambda)e^{C/\sqrt{\lambda}} + \lambda} \right)^{-1}. \quad (26)$$

At the point  $C = 0$  the result is

$$\langle s \rangle \approx \frac{2(1-\lambda)}{\sqrt{\pi\lambda N}} \left( 1 - \frac{1-2\lambda}{4} \sqrt{\frac{\pi}{\lambda N}} \right). \quad (27)$$

For the strongly repulsive regime ( $-\gamma \gg 1$ ) the average number of contacts  $\langle S \rangle$  is independent of  $N$  and quite small:

$$\langle S \rangle \approx 1 - \frac{1-\lambda}{C\sqrt{\lambda}}. \quad (28)$$

Figure 3 shows the dependence of  $\langle s \rangle$  on the adsorption interaction parameter  $C$  in the adsorption regime for a long polymer chain of  $N = 10\,000$ . The data points represent results of lattice calculations for several lattices, the solid curves correspond to ground-state equation (26). It can be

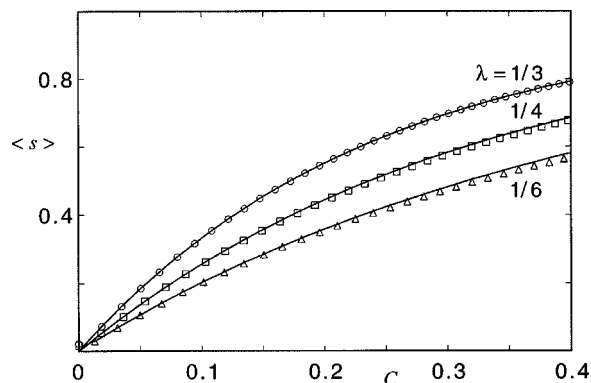


FIG. 3. The average fraction of adsorbed units  $\langle s \rangle$  as a function of the adsorption interaction parameter  $C$  for a polymer chain of  $N = 10\,000$  segments obtained from lattice calculations (points), and from the ground-state continuum equation (26) (solid curves), for three lattice types.

seen that in the case of large  $N$  the results obtained for the continuum and lattice model practically coincide for all  $\lambda$ .

The dependencies of  $\langle s \rangle$  on  $\chi_s$  over the whole range of  $C$  for various  $N$  values and the simple cubic lattice are shown in Fig. 4. Again points represent results of lattice model calculations, and the full curves correspond to the general continuum model equations (25) and (13). As can be seen in Fig. 4 these equations describe the numerical results, obtained for the lattice model at both large and small  $N$ , very well. The dashed and dotted curves show the results for  $\langle s \rangle$  obtained by substituting Eqs. (19) and (20), respectively, into Eq. (25). These expressions for the three regimes describe the numerical results for  $N = 10$  rather well and those for  $N = 100$  very well. The average fraction of surface contacts has a kink as a function of  $\chi_s$  for an infinitely long chain, demonstrating that there is a second-order phase transition in the critical point.

We now consider how the chains are distributed according to the number of their contacts with the surface. A scaled form of the contact number distribution function was obtained in Ref. 34 from analyzing the symmetry properties of a more general polymer model, in which an external force

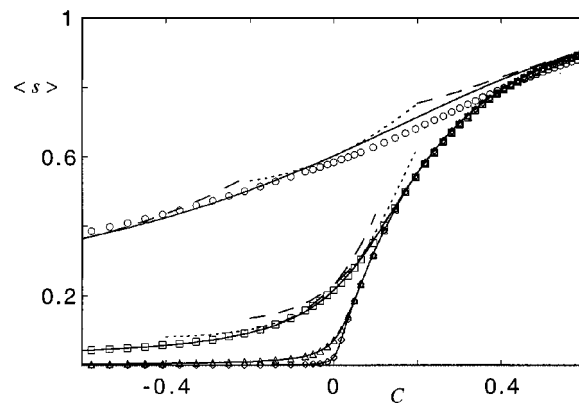


FIG. 4. Dependence of  $\langle s \rangle$  on  $C$  for  $\lambda = 1/6$  at  $N = 10$  (circles), 100 (squares), 1000 (triangles), and 10 000 (diamonds). Points are lattice calculations, the full curves were obtained from Eq. (25). Dashed curves are asymptotes for  $N \rightarrow \infty$  obtained with Eq. (19) substituted into Eq. (25); these asymptotes merge with the full curves for large  $|C|$ . The dotted curves correspond to the expansion for finite  $N$  around  $C = 0$  [Eq. (20)].

was applied to the free chain end. According to this analysis, the statistical weight  $P_{\text{cont}}(M)$  for chains with a given scaled number of contacts  $M$  is a Gaussian function of the parameter  $M$ :

$$P_{\text{cont}}(\gamma, M) = \frac{2e^{\gamma^2}}{\sqrt{\pi}} \cdot e^{-(M-\gamma)^2}. \quad (29)$$

The integral of the function  $P_{\text{cont}}(\gamma, M)$  over all  $M$  gives again the full partition function  $Q(\gamma)$ . Using Eq. (24) in the form

$$S = \frac{\partial c}{\partial \chi_s} 2R \cdot M \quad (30)$$

it is possible to transform the contact number distribution function calculated for any lattice into the scaled form of Eq. (24). The first moment of the contact distribution function gives the average fraction of the surface contacts, coinciding, of course, with Eq. (25).

Figures 5(a)–5(c) show the distribution functions  $W_{\text{cont}}(S) = P_{\text{cont}}(S)/Q$  (which is normalized to unity) for a simple cubic lattice at  $\chi_s = 0$  ( $C = -1/\sqrt{6} \approx -0.408$ ), at  $\chi_s = \chi_{sc} = \ln(6/5)$  ( $C = 0$ ), and at  $\chi_s = 0.25$  ( $C \approx 0.122$ ). Points represent the contact number distributions calculated for a simple cubic lattice model. The details of these lattice calculations are described in the appendix. The full curves in Fig. 5 correspond to Eq. (29).

It is clear from Figs. 5(a)–5(c) that the agreement between Eq. (29) and the numerical data is excellent. Note that the abscissa axis is rescaled for  $\chi_s = \chi_{sc}$  and  $\chi_s = 0.25$ , in order to ensure that the data for different chain lengths coincide. In the lattice calculation for  $\chi_s = 0$  and  $N = 10$  [Fig. 5(a)] the probability for a fully adsorbed chain ( $S = 10$ ) is higher than for  $S = 9$ . This effect is also present for higher chain lengths (not shown). It is a lattice artifact, which becomes less pronounced and eventually disappears when  $\lambda$  is increased. For positive adsorption energies, the lattice results for  $N = 10$  deviate rather strongly, therefore they are omitted from Figs. 5(b) and 5(c).

## VI. DISTRIBUTION OF TAIL LENGTHS, THE AVERAGE TAIL LENGTH, AND ITS FLUCTUATION

The statistical weight  $P_{\text{tail}}(T)$  for chains of  $N$  segments having a given number  $T$  of segments in a free tail can be easily constructed using the known expressions for the fixed-end partition function  $P$  and for the free end partition function  $Q$ , since  $P_{\text{tail}}$  is expressible in terms of the product  $P(0, N-T, C) \cdot Q(T, C \rightarrow -\infty)$ . The result, normalized to  $Q_N = Y(-\gamma)$ , can be written as

$$P_{\text{tail}}(\gamma, t) = \frac{1}{\pi\sqrt{t(1-t)}} + \frac{\gamma}{\sqrt{\pi}} \cdot \frac{Y(-\gamma\sqrt{1-t})}{\sqrt{t}}, \quad (31)$$

where  $t \equiv T/N$  is the fraction of tail segments. In Fig. 6 we present several examples of the tail length distribution function,  $W_{\text{tail}}(t) = P_{\text{tail}}(t)/Q$ , where  $W_{\text{tail}}(t)$  is thus normalized to unity. The solid curves in Figs. 6(a)–6(d) correspond to Eq. (31).

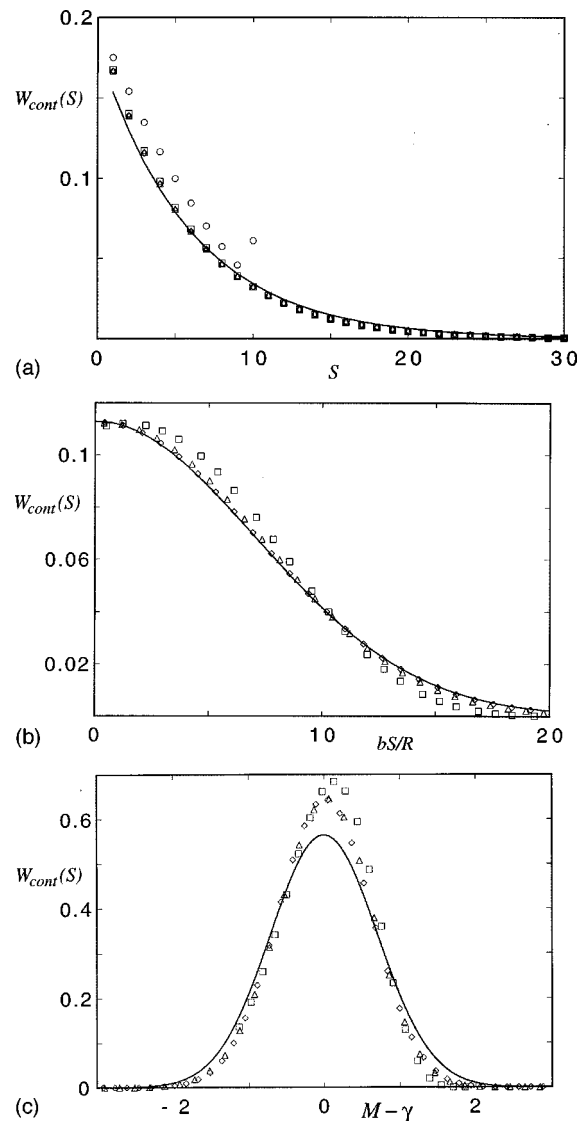


FIG. 5. Contact number distribution functions  $W_{\text{cont}}(S)$  calculated for a simple cubic lattice ( $\lambda = 1/6$ ) at three different surface interaction parameters. The points represent lattice calculations, with the same symbols as in Fig. 4. The curves correspond to Eq. (29) normalized with  $Q$ . (a) Repulsive case ( $\chi_s = 0$ ); (b) Adsorption threshold point ( $\chi_s = \chi_{sc}$ );  $W_{\text{cont}}$  is now plotted as a function of the parameter  $bS/R$ ; (c) Adsorption regime ( $\chi_s = 0.25$ ); here  $W_{\text{cont}}$  is plotted against the scaled coordinates  $M - \gamma$ .

Near the multicritical point, where  $|\gamma| \ll 1$ , Eq. (31) can be approximated as

$$P_{\text{tail}}(\gamma, t) \approx \frac{1}{\pi\sqrt{t(1-t)}} + \frac{\gamma}{\sqrt{\pi}\sqrt{t}} + \frac{2}{\pi} \gamma^2 \cdot \sqrt{\frac{1-t}{t}}. \quad (32)$$

The first term in Eq. (32) corresponds to the point  $c = 0$ . A very interesting feature of the tail distribution function at  $c = 0$  is its bimodal character [see Fig. 6(a)]. This means that there are two dominating chain populations, one with few loops and a long tail, and the other with long loops and a very short tail. As can be seen from Eqs. (31) and (32) and from the plots in Fig. 6 the function  $P_{\text{tail}}$  stays bimodal not only for  $|\gamma| < 1$  but even at high (both positive and negative) values of  $\gamma$ .

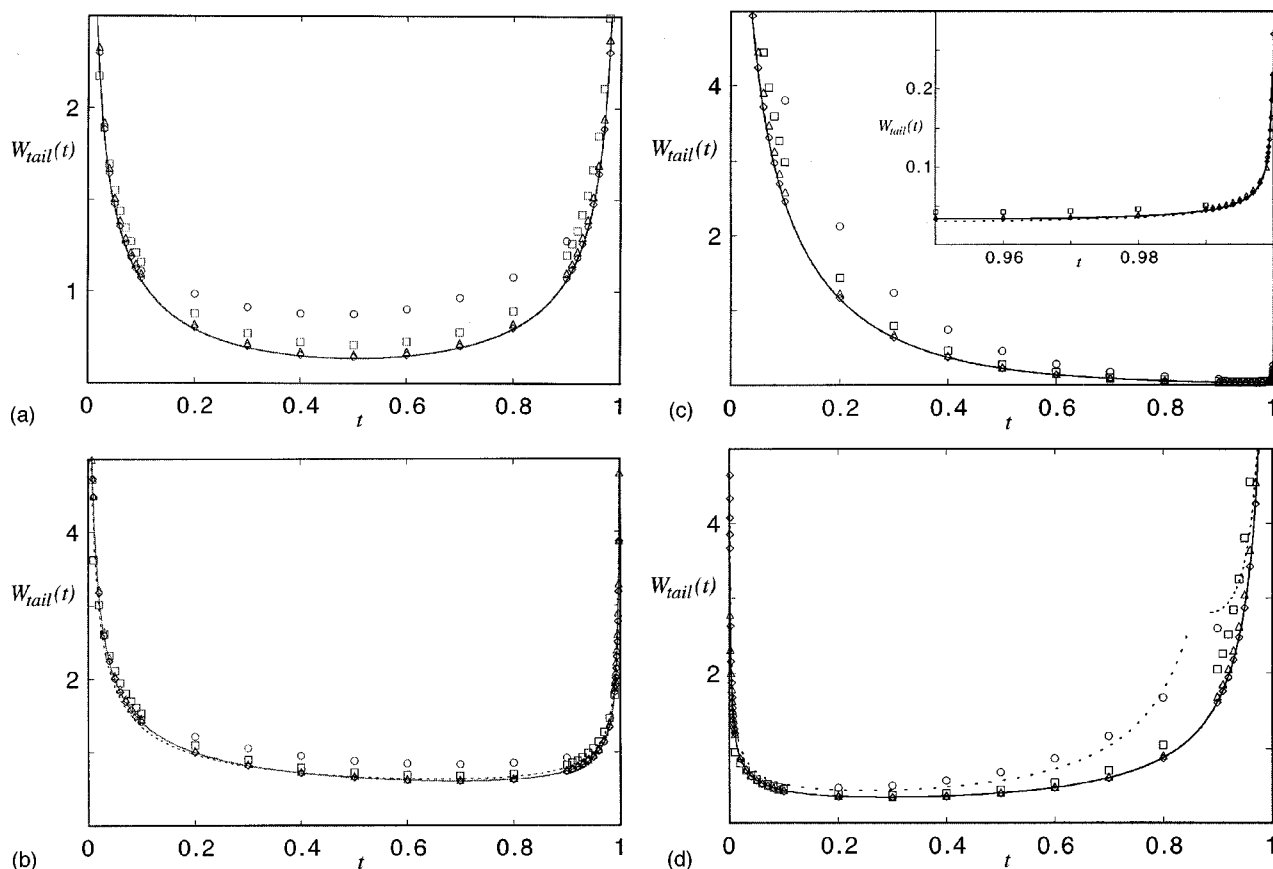


FIG. 6. The distribution function  $W_{\text{tail}}(t)$  for an end-attached chain having a given portion of segments  $t=T/N$  in the free tail, calculated for four different values of the surface interaction. Points represent lattice calculations for a simple cubic lattice model,  $\lambda=1/6$ . Different chain lengths are denoted as in Fig. 4. The solid curves correspond to Eq. (31). Values of the continuum model surface interaction parameter  $C$  are chosen such as to keep the product  $\gamma \equiv C\sqrt{N}$  constant; the corresponding values of the lattice model interaction parameter  $\chi_s$  are calculated using Eq. (17). (a) Critical point ( $\gamma=0$ ); (b) a case of weak adsorption interaction ( $\gamma=0.5$ ); the dotted curve represents the approximate equation (32). (c) Ground-state adsorption regime ( $\gamma=2$ ); the inset shows the region of  $t$  close to unity, with the dotted curve calculated from Eq. (32); (d) Repulsive regime ( $\gamma=-2$ ); the dotted curve to the left represents the small- $t$  asymptote Eq. (34), the dotted curve to the right corresponds to Eq. (32).

For  $\gamma > 1$ , the function  $P_{\text{tail}}$  for nearly the whole  $t$  interval (i.e., for  $0 < t < 1 - \gamma^{-2}$ ) reduces to

$$P_{\text{tail}}(\gamma, t) \approx \frac{2\gamma e^{\gamma^2}}{\sqrt{\pi t}} e^{-\gamma^2 t} = 2C \sqrt{\frac{N}{\pi t}} \cdot 2e^{C^2 N(1-t)}. \quad (33)$$

According to this equation  $P_{\text{tail}}$  is a monotonically decreasing function of  $t$ ; it coincides with the ground-state result.

It is interesting to note, however, that for  $t$  values exceeding  $1 - \gamma^{-2}$  the general Eq. (31) reduces to Eq. (32), causing  $P_{\text{tail}}(t)$  to increase with  $t$  in this small interval of  $t$ . This feature of the tail length distribution function cannot be derived from the ground-state approach. Since this effect is quite small for  $\gamma \gg 1$  [see Fig. 6(c)] it does not have any practical influence on the average behavior of a terminally attached polymer molecule in the adsorption regime, being only an interesting small detail in the whole picture.

For  $-\gamma > 1$  the function  $P_{\text{tail}}(t)$  can be roughly approximated as

$$P_{\text{tail}}(\gamma, t) \approx \frac{1}{2\pi\gamma^2 \sqrt{t(1-t)^3}}, \quad (34)$$

Eq. (34) describes the distribution for  $t < 1 - \gamma^{-2}$ ; for higher  $t$  values (close to unity) we should again use Eq. (32) instead of Eq. (34).

We also calculated the distribution function  $W_{\text{tail}}(t)$  for the simple cubic lattice model with  $N$  values equal to 10, 100, 1000, and 10000 and different values of the  $\chi_s$  parameter, chosen in such a way as to maintain a constant  $\gamma = C\sqrt{N}$ . The limiting Eq. (17) was used to calculate these  $\chi_s$  values. The lattice results are shown as data points in Figs. 6(a)–6(d). As stated above, the solid curves represent the full continuum model tail distribution function, Eq. (31), and the dashed or dotted curves correspond to the appropriate asymptotic expansions. The inset in Fig. 6(c) shows the increasing part of  $W(t)$  in the case of  $\gamma=2$  for  $t$  values close to unity.

As can be seen in Fig. 6, in all cases the lattice data for  $N > \approx 100$  are very close to Eq. (31) of the continuum model. The data for  $N=10$  deviate somewhat, which is partly caused by using Eq. (17) (applying only for  $N \rightarrow \infty$ ) for calculating  $\chi_s$  from  $c$ ; applying Eq. (13) would have given better agreement for (very) short chains, especially for  $\gamma=0$ . All the asymptotic expansions also look quite reasonable.

We performed calculations of the function  $W(t)$  with



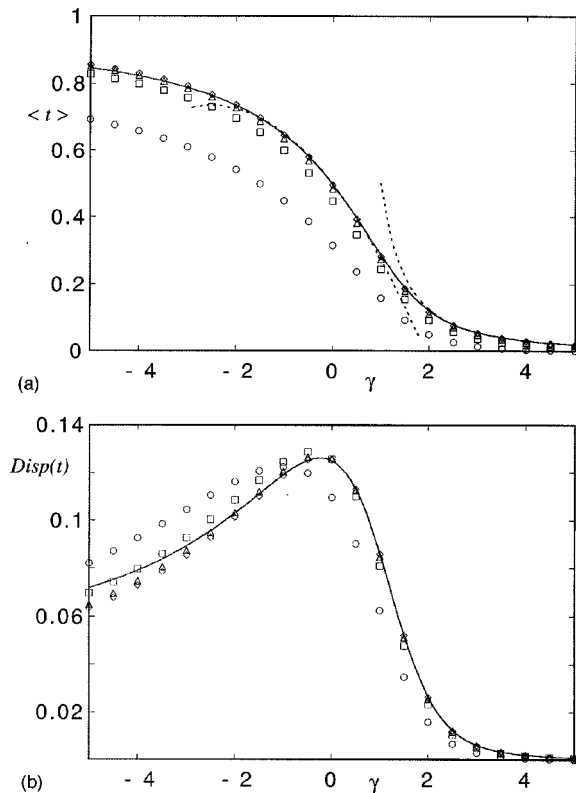


FIG. 7. (a) The average fraction of tail segments  $\langle t \rangle$  and (b) the dispersion of the fraction of tail segments  $Disp(t)$  as a function of the scaled surface interaction parameter  $\gamma = C\sqrt{N}$ . The points represent lattice data like in Fig. 4, the solid curve corresponds to the general equation (31), and the dotted curves represent the ground-state asymptote and the expansion around  $\gamma = 0$ .

different lattice types. The data in Fig. 6 are for  $\lambda = 1/6$ . Other lattice constants  $\lambda$  yield essentially identical results: there are minute numerical differences which are, however, hardly visible in a graph. Therefore we do not show these data separately.

We now consider briefly the moments of the function  $P_{\text{tail}}(\gamma, t)$ . The first moment is equal to the average fraction of chain units in the tail  $\langle t \rangle$  and is also related to average tail length  $\langle T \rangle$  through  $\langle t \rangle \equiv n_t \langle T \rangle / N$ , where  $n_t$  is the average number of tails per chain. The dependence of  $\langle t \rangle$  on  $\gamma = C\sqrt{N}$  according to Eq. (31) is shown in Fig. 7(a) (solid curve). Some typical lattice data are also given (data points). Again the agreement is excellent for  $N = 100$ . Note that the average number of tails  $n_t$  is unity in the continuum model, because the probability of finding the end of the chain *exactly* at coordinate  $z = 0$  is zero. This is in contrast with the lattice model where all segments could be in layer  $z = 0$  so there is a finite probability of finding no tail at all:  $n_t$  in the lattice model is smaller than unity, especially so for small  $N$  and high  $\chi_s$ .

Using the expansions of Eq. (9) for the function  $Y(x)$  one can easily derive that in the ground-state adsorption regime ( $\gamma \gg 1$ ) the average number of chain segments in the tail  $\langle T \rangle = N \langle t \rangle$  does not depend on the chain length  $N$ , and is equal to  $1/(2C^2)$ . Hence, in this region  $\langle t \rangle = 1/(2\gamma^2)$ . This asymptotic behavior is shown in Fig. 7(a) as the dashed curve to the right; it is accurate down to  $\gamma = 2$ .

Another interesting case is  $C = 0$  where we have the

well-known result<sup>15</sup> that on average one-half of the chain forms a tail. In the vicinity of the multicritical point, at  $|\gamma| \ll 1$ , we find

$$\langle t \rangle = \frac{1}{2} - \frac{1}{3\sqrt{\pi}} \gamma - \frac{3\pi - 8}{12\pi} \gamma^2. \quad (35)$$

This dependence is shown as the dotted curve in Fig. 7(a), and is accurate in the interval  $-1 < \gamma < 1$ .

When  $C$  becomes negative, at  $-\gamma \gg 1$ ,  $\langle t \rangle$  tends to unity, and the number of segments in trains and loops,  $N - \langle T \rangle$ , is then quite small. This number does not depend on chain length, and is only a function of the  $C$  parameter.

Also the fluctuations in the tail length can be estimated using the second moment of the function  $P_{\text{tail}}(\gamma, t)$ . In particular, at  $C = 0$  we have  $Disp(t) = \langle t^2 \rangle - \langle t \rangle^2 = 1/8$ , which means that at  $C = 0$  the fluctuation in the tail length,  $\delta(T) = N\sqrt{Disp(t)}$ , is proportional to the average tail length  $\langle T \rangle$  according to  $\delta(T) = \langle T \rangle / \sqrt{2}$ , so that the relative fluctuation is equal to  $1/\sqrt{2}$ . In the ground state regime  $Disp(t) = 1/(2\gamma^4)$  and the relative fluctuation is equal to  $\sqrt{2}$ . The function  $Disp(t)$  is shown as a function of the parameter  $\gamma$  in Fig. 7(b). Again the agreement with the lattice data is excellent for  $N \geq 100$ .

In the limit  $N \rightarrow \infty$  the average fraction of tail segments  $\langle t \rangle$  as a function of  $C$  turns into a step function, while the dispersion will have only one nonzero value of  $1/8$  at the point  $C = 0$ .

## VII. CONCLUSION

We presented a general equation relating the adsorption interaction parameter  $\chi_s$  in a lattice model to the extrapolation length  $1/c$  in a continuum model for a polymer chain of finite length interacting with a planar surface. We use a dimensionless adsorption parameter  $C \equiv bc/\sqrt{6}$ , where  $b$  is the bond length. If the radius of gyration  $R$  is much higher than the lattice spacing  $l = b/\sqrt{6\lambda}$  (which condition is practically fulfilled when the number of the chain segments  $N$  is of order 100) this general equation reduces to the simple relation (17) which is independent of  $N$  and contains only the lattice parameter  $\lambda$ . For a short chain ( $N < 100$ ) this simple formula (17) also holds provided that  $|C|\sqrt{N} \gg 1$ , which is the case when the surface interaction energy is not very close to its critical value ( $C = 0$ ).

At  $|C|\sqrt{N} < 1$  (short chains and close to the point  $C = 0$ ) the relation between  $\chi_s$  and  $C$  becomes dependent on the number of chain units  $N$ , which means that the continuum model in this case is not fully equivalent to the lattice model. It is possible, however, to relate  $\chi_s$  and  $C$  even in this case by considering this relationship as an  $N$ -dependent function and using the general equation (13) or its appropriate expansions around  $C \approx 0$  instead of Eq. (17). In doing so we obtained excellent agreement between the lattice and continuum results even for short polymer chains in the vicinity of the critical point. This analysis also yielded an explicit expression, Eq. (16), for the (weak) dependence on the chain length of the (lattice) adsorption energy  $\chi_s$  at the point where the adsorption/desorption transition occurs.

We applied the relation between  $\chi_s$  and  $C$  for describing structural features of an ideal chain anchored to a planar surface. Two features were discussed in some detail: parameters related to the number of contacts between the chain and the surface (“trains”), and those related to the number of units in terminal chain fragments having no surface contacts (“tails”).

For the tail-related properties we obtained continuum equations which contain as the only parameter the product  $\gamma=cR=C\sqrt{N}$ . This product is independent of the microscopic details of the polymer chain and the adsorbing surface. We demonstrated that these tail-related properties are indeed model-independent: calculations for different lattice types at constant  $\gamma=cR$  show that these properties do not depend on the lattice parameter  $\lambda$ .

Such universality does not apply for properties related to the number of surface contacts. The equations for the surface contacts contain, apart from universal terms originating from the continuum model, also a nonuniversal factor depending on microscopic details of polymer-surface interaction. We derived an equation for calculating this nonuniversal factor for different lattice models and demonstrated excellent agreement between the lattice results and the continuum model.

## ACKNOWLEDGMENTS

This work was performed in the framework of a bilateral cooperation between the Dutch Organization for Scientific Research (NWO) and Russia, in the Program “Polymer Physics in Food Science.” A.M.S. acknowledges support from the Russian Fund of Fundamental Investigations, Grant No. 9903-33385a.

## APPENDIX: LATTICE CALCULATION OF CONTACT NUMBER DISTRIBUTIONS

The contact number distribution function  $W_{\text{cont}}(S)$  gives the probability of finding a chain with  $S$  surface contacts. To obtain this function first a set of end-point distribution functions  $P_S(z,n)$  is defined. These are a measure for the probability of a walk that starts at the surface and ends after  $n$  steps (segments) in layer  $z$ , under the condition of  $S$  surface contacts. The functions  $P_S(z,n)$  are calculated with the following recurrence relations, similar to Eqs. (2) and (3):

$$P_S(0,n+1) = (1-2\lambda)P_{S-1}(0,n) + \lambda P_{S-1}(l,n),$$

$$P_S(z,n+1) = \lambda P_S(z-l,n) + (1-2\lambda)P_S(z,n) + \lambda P_S(z+l,n).$$

The starting condition reads  $P_1(0,1) = 1$  with all other values set to zero. At the end of the propagator procedure, i.e., when  $n=N$ , the contact number distribution function is calculated as

$$W_{\text{cont}}(S) = \frac{\exp(-S\chi_S) \sum_z P_S(z,N)}{\sum_{z,S} P_S(z,N) \exp(-S\chi_S)}.$$

Note that it is only necessary to compute  $P_S(z,N)$ , the computationally most demanding task, for  $\chi_s=0$ : the adsorption energy is incorporated through Boltzmann weighting.

- <sup>1</sup>P. G. de Gennes, *Scaling Concepts in Polymer Physics* (Cornell University Press, Ithaca, NY, 1979).
- <sup>2</sup>K. Binder, in *Phase Transitions and Critical Phenomena*, edited by C. Domb and J. L. Lebowitz (Academic, London, 1986), Vol. 8, p. 1.
- <sup>3</sup>G. J. Fleer, M. A. Cohen Stuart, J. M. H. M. Scheutjens, T. Cosgrove, and B. Vincent, *Polymers at Interfaces* (Chapman and Hall, London, 1993).
- <sup>4</sup>D. H. Napper, *Polymeric Stabilization of Colloidal Dispersions* (Academic, London, 1989).
- <sup>5</sup>*Physics of Polymer Surfaces and Interfaces*, edited by I. C. Sanchez (Butterworth-Heinemann, Boston, 1992).
- <sup>6</sup>P. A. Pincus, C. J. Sandroff, and T. A. Witten, *J. Phys. (Paris)* **45**, 725 (1984).
- <sup>7</sup>E. F. Casassa, *J. Polym. Sci., Part B: Polym. Lett.* **5**, 773 (1967); *Macromolecules* **9**, 182 (1976); E. F. Casassa and Y. Tagami, *ibid.* **2**, 14 (1969).
- <sup>8</sup>A. M. Skvortsov and A. A. Gorbunov, *J. Chromatogr.* **358**, 77 (1986); **507**, 487 (1990); A. Gorbunov, A. Skvortsov, B. Trathnigg, M. Kollroser, and M. Parth, *ibid.* **798**, 187 (1998).
- <sup>9</sup>E. A. DiMarzio, C. M. Guttman, and A. Mah, *Macromolecules* **28**, 2930 (1995); C. M. Guttman, E. A. DiMarzio, and J. F. Douglas, *ibid.* **29**, 5723 (1996).
- <sup>10</sup>H. L. Frisch, R. Simha, and F. R. Eirich, *J. Chem. Phys.* **21**, 365 (1953); *J. Phys. Chem.* **57**, 584 (1953).
- <sup>11</sup>A. Silberberg, *J. Phys. Chem.* **66**, 1872 (1962); *J. Chem. Phys.* **46**, 1105 (1967).
- <sup>12</sup>C. A. J. Hoeve, E. A. DiMarzio, and P. Peyser, *J. Chem. Phys.* **42**, 2558 (1965); C. J. Hoeve, *J. Polym. Sci., Part C: Polym. Symp.* **30**, 361 (1970).
- <sup>13</sup>R. J. Roe, *J. Chem. Phys.* **43**, 1591 (1965); **44**, 4264 (1966).
- <sup>14</sup>E. A. DiMarzio, *J. Chem. Phys.* **42**, 2101 (1965); E. A. DiMarzio and F. L. McCrackin, *ibid.* **43**, 539 (1965).
- <sup>15</sup>R. J. Rubin, *J. Res. Natl. Bur. Stand., Sect. B* **69**, 301 (1965); **70**, 237 (1965); *J. Chem. Phys.* **43**, 2392 (1965).
- <sup>16</sup>E. Eisenriegler, *Polymers Near Interfaces* (World Scientific, Singapore, 1993).
- <sup>17</sup>A. A. Gorbunov and A. M. Skvortsov, *Adv. Colloid Interface Sci.* **62**, 31 (1995).
- <sup>18</sup>G. H. Weiss and R. J. Rubin, *Adv. Chem. Phys.* **52**, 363 (1983); R. J. Rubin, in *Random Walks and their Applications in Physical and Biological Sciences*, AIP Conference Proceedings Series 109, edited by M. F. Schlesinger and B. J. West (NBS-La Jolla Institute, CA, 1982), p. 73.
- <sup>19</sup>E. J. Clayfield and E. C. Lumb, *J. Colloid Interface Sci.* **22**, 284 (1966).
- <sup>20</sup>F. L. McCrackin, *J. Chem. Phys.* **47**, 1980 (1967).
- <sup>21</sup>E. Eisenriegler, K. Kremer, and K. Binder, *J. Chem. Phys.* **77**, 6296 (1982).
- <sup>22</sup>Y. Lepine and A. Caille, *Can. J. Phys.* **56**, 403 (1978).
- <sup>23</sup>A. M. Nemirovsky and K. F. Freed, *J. Chem. Phys.* **83**, 4166 (1985); Z.-G. Wang, A. M. Nemirovsky, and K. F. Freed, *ibid.* **86**, 4266 (1987).
- <sup>24</sup>G. Stratouras and M. K. Kosmas, *Macromolecules* **24**, 6754 (1991); *J. Chem. Phys.* **95**, 4656 (1991); **102**, 2239 (1995).
- <sup>25</sup>A. A. Gorbunov and A. M. Skvortsov, *Vysokomol. Soedin., Ser. A* **31**, 1244 (1989).
- <sup>26</sup>G. J. Fleer, J. van Male, and A. Johner, *Macromolecules* **32**, 825 (1999); **32**, 845 (1999).
- <sup>27</sup>A. M. Skvortsov, A. A. Gorbunov, F. A. M. Leermakers, and G. J. Fleer, *Macromolecules* **32**, 2004 (1999).
- <sup>28</sup>J. M. H. M. Scheutjens and G. J. Fleer, *J. Phys. Chem.* **83**, 1619 (1979); **84**, 178 (1980).
- <sup>29</sup>S. Chandrasekhar, *Rev. Mod. Phys.* **15**, 1 (1943).
- <sup>30</sup>P. G. deGennes, *Rep. Prog. Phys.* **32**, 187 (1969).
- <sup>31</sup>L. I. Klushin, A. M. Skvortsov, and A. A. Gorbunov, *Phys. Rev. E* **56**, 1511 (1997).
- <sup>32</sup>L. A. Meijer, F. A. M. Leermakers, and J. Lyklema, *J. Phys. Chem.* **99**, 17282 (1995).
- <sup>33</sup>E. Eisenriegler, A. Hanke, and S. Dietrich, *Phys. Rev. E* **54**, 1134 (1996).
- <sup>34</sup>A. M. Skvortsov, A. A. Gorbunov, and L. I. Klushin, *J. Chem. Phys.* **100**, 2325 (1994).